Materials Research Bulletin 105 (2018) 121–125

Contents lists available at ScienceDirect

Materials Research Bulletin

journal homepage: www.elsevier.com/locate/matresbu

Structural, morphological, optical and magnetic properties of $Ag_{3(2+x)}In_xNb_{4-x}O_{11+\delta}$ ($0.25 \leq x \leq 1.0$) nanoparticles synthesized by sol–gel method

S. Ramesh[a,b,*], Jerald V. Ramaclus[c], B.B. Das[d], Edgar Mosquera[a,e]

[a] Laboratorio de Materiales Funcionales a Nanoescala, Departamento de Ciencia de los Materiales, Universidad de Chile, Beauchef 851, Santiago, Chile
[b] Saveetha School of Engineering, Saveetha University, Chennai, 602105, India
[c] Department of Physics, St. Joseph's College, Tiruchirappalli, Tamil Nadu, 620002, India
[d] Department of Chemistry, Pondicherry University, Pondicherry, 605014, India
[e] Departamento de Física, Universidad del Valle, A.A. 25360, Cali, Colombia

ARTICLE INFO

Keywords:
Sol-gel preparation
Nanoparticles
Semiconductors
Magnetic materials

ABSTRACT

Herein, we report the structure, morphology, optical and magnetic properties of novel $Ag_{3\ (2+x)}\ In_xNb_{4-x}O_{11+\delta}$ ($0.25 \leq \times \leq 1.0$; A1–A4) nanoparticles prepared by sol-gel technique. The samples were studied using X-ray diffraction, electron microscopy, diffuse reflectance spectroscopy, vibrating sample magnetometer, and electron spin resonance. X-ray diffraction studies confirm the formation of monoclinic lattice type with P2/m space group. Purity and homogeneity of the samples were confirmed by X-ray mapping. The semiconductor nature of the samples was identified by optical absorption spectra which indicate an inter-band transition from the oxygen 2p to niobium 4d electronic states. The magnetization plots reveal the room temperature ferromagnetic behavior of the samples.

1. Introduction

Silver-niobium based compounds have been widely investigated multifunctional materials for the promising applications as ferroelectrics, piezoelectrics, thermoelectrics, dye-sensitized solar cells, catalysis, optical devices and degradation of organic pollutants [1–4]. The properties of niobium oxide can be tailored according to the desired application simply by doping of metal and non-metals, in particular, the doping of noble metals like silver into niobium oxide is expected to increase the carrier mobility. This relatively higher delocalization of 3d orbitals may share in hybridization of the energy band structure which inturn increases the catalytic activity [5]. Recently, several series of niobium incorporating multifunctional metal oxides with the general formula of $A_{n+1}B_nO_{3n+1}$, $AA'_{n-1}Nb_nO_{3n+1}$ (A = K, Rb, Cs, Cu; A' = Bi, Ba, Pr, la), $Ag_{3(2+x)}Pr_x\ Nb_{4-x}O_{11+\delta}$, $A_nNb_{3n+1}O_{8n+3}$ (A = Ca, Na, K, Cu, Ag) are found to exhibit different properties like ferroelectrics, photocatalysis and phase transitions [6–9]. On the other hand, Indium oxide (In_2O_3), is a commonly used compound in the applications of transistors, sensors [10], solar cells [11,12], photocatalysis [13], field emission devices and window heaters [14]. It is generally used as a dopant to generate charge carriers of suffucient quantity to increase the electrical conductance of solar cells [15–17]. Therefore the combination of silver, indium and niobium oxides can result in interesting multifuctional properties which have not yet been investigated. One of the possibility when indium is integrated into silver-niobium system is, to improve the charge carriers which may help to further increase electrical conductivity of the system [16]. Thus, Ag_2O, Nb_2O_5, and In_2O_3 are excellent candidates for multifunctional nanomaterials for meeting the requirements of advanced science applications in the future. In our previous work, $Ag_{3(2+x)}Pr_xNb_{4-x}O_{11+\delta}$ was identified as stable multiferroic material. Therefore, in this article, we report a sol-gel synthesis route for obtaining $Ag_{3(2+x)}In_xNb_{4-x}O_{11+\delta}$ ($0.25 \leq \times \leq 1.0$; A1-A4) nanoparticles for the first time and study their optical absorbance, electrical and magnetic properties, at room temperature.

2. Experimental

2.1. Synthesis of $Ag_{3(2+x)}In_xNb_{4-x}O_{11+\delta}$ ($0.25 \leq \times \leq 1.0$) nanoparticles

Nanocrystalline $Ag_{3(2+x)}In_xNb_{4-x}O_{11+\delta}$ ($0.25 \leq \times \leq 1.0$) samples are prepared using sol-gel technique. Reagents are used without purification. Niobium citrate was synthesized using the required quantity of niobium oxide as described in our previous paper [5]. Niobium

* Corresponding author at: Laboratorio de Materiales Funcionales a Nanoescala, Departamento de Ciencia de los Materiales, Universidad de Chile, Beauchef 851, Santiago, Chile.
E-mail address: rsivasamy@ing.uchile.cl (R. S.).

https://doi.org/10.1016/j.materresbull.2018.04.049
Received 30 May 2017; Received in revised form 9 April 2018; Accepted 27 April 2018
Available online 30 April 2018
0025-5408/

citrate, indium and silver nitrate solutions were mixed and stirred for 1 h then 1.5 M citric acid solution of 30 ml were added into the resulting the solution mixture. The pH of the solution is maintained at 6 using liquid ammonia. The above solution is stirred continuously at 333 K till it converts a clear gel. The gel was broken at 473 K for 1 h. Finally, sintered for 4 h at 1123 K to achieve a well homogeneous condensed powder. The systematic preparation of the nanoparticles and the calculated amount of precursors aregiven in the supplementary information.

2.2. Characterization

The room temperature X-ray diffraction (PXRD) patterns were recorded by X'Pert PANalytical X-ray diffractometer in Bragg-Brentano configuration with monochromatic Cu Kα radiation (Cu Ka 1, 2 (λ ~ 1.54060, 1.54443 A), as a source and 40 kV/30 mA power. A scanning electron microscope (SEM) Hitchi-S3400 was used to investigate the morphology of the samples. The SUPER DRYER II was used to identify the element compositions and its distribution. The thermal analysis was done using TA Q600 SDT in the temperature range of 50–1000 °C at 10 °C/s under the N_2 atmosphere. The optical absorption spectra by a Varian Cary 5000 UV–VIS spectrometer. Magnetic properties by a LAKESHORE VSM 7404 vibrating sample magnetometer (VSM). The electron spin resonance (ESR) experiments at 77 and 300 K were performed with a JEOL JES-TE 100 ESR spectrometer at 100 kHz field modulation and magnetic field calibration was made with respect to the resonance line of DPPH (g_{DPPH} = 2.0035) as a field marker [18].

3. Results and discussion

3.1. X-ray diffraction studies

Powder X-ray diffraction patterns of $Ag_{3(2+x)}In_xNb_{4-x}O_{11+\delta}$ ($0.25 \leq \times \leq 1.0$; A1–A4) nanoparticles with corresponding (*hkl*) planes are shown in Fig. 1. In PXRD patterns, all the principal peaks are at the same diffraction angle which confirms the single-phase polycrystalline nature of the samples. The structural analysis was obtained using FullProf package. The least-squares procedure was used to index the diffraction peaks. The XRD result of A1–A4 shows comparable lattice parameters of the monoclinic lattice type with P2/m space group. To study the effect of In ions concentration, we pay attention to the XRD patterns the three peaks at 38°, 44° and 64° increases with increasing concentration of In ions. Similarly, the peak at 46° reduces from A1-A4, indicates the reducing the concentration of Nb ions in the samples. The average crystallite sizes were calculated from the XRD patterns by the Debye-Scherrer and Williamson-Hall methods [19,20]. The methods (1) and (2) are shown below

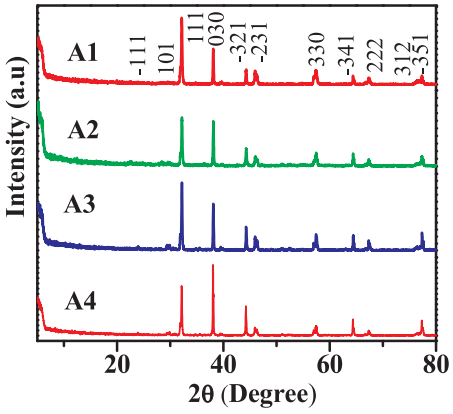

Fig. 1. XRD patterns of $Ag_{3(2+x)}In_xNb_{4-x}O_{11+\delta}$ ($0.25 \leq \times \leq 1.0$; A1–A4) nanoparticle.

Table 1
Lattice parameters, crystallite sizes, magnetic properties of $Ag_{3(2+x)}In_xNb_{4-x}O_{11+\delta}$ ($0.25 \leq \times \leq 1.0$; A1–A4) nanoparticles.

Sample code		A1	A2	A3	A4
Lattice type		Mono	Mono	Mono	Mono
a (Å)		7.5074	7.5063	7.5050	7.5124
b (Å)		7.0800	7.0764	7.0776	7.0864
c (Å)		5.0018	4.9984	5.0041	4.9947
β		119.09	119.11	119.14	119.00
Unit cell volume		232.30	231.96	232.15	232.54
Space group		P2/m	P2/m	P2/m	P2/m
Crystallite Size (nm)	Scherer	23.0	24.3	21.3	19.9
	WH Plot	26.7	23.2	25.1	26.4
χ x10⁻5 (emu/gG)		1.08	2.17	21.35	12.01
H_{ci} (G)		175.92	222.20	148.42	241.15
M_s (emu/g)		0.027	0.021	0.037	0.046
$M_r \times 10^{-3}$(emu/g),		0.60	0.73	1.09	1.69
g matrix	300 K	2.0368	2.0225	2.0099	2.0001
	77 K	2.0310	2.0302	2.0012	2.0301

Mono = Monoclinic.

$$D = 0.89\lambda/\beta_1/2\cos\theta_{hkl} \quad (1)$$

$$\beta\cos\theta = K\lambda/D + 2\varepsilon\sin\theta \quad (2)$$

Where D- crystallite size, λ- wavelength of Cu Kα radiation, β- half-width of the diffraction peak, θ- Bragg angle, K- Scherer constant, and ε-lattice strain. It is realized that the average crystallite sizes are increasing with increasing content of the In^{3+} ion. The increasing crystallite size is due to the change in higher ionic radius of In^{3+} (94 pm) ions with the smaller Nb^{4+} (82 pm) ions. The lattice parameters and crystallite sizes are reported in Table 1.

3.2. Morphology analysis

Morphological examinations were executed by SEM, and quantitative analysis by the EDS profile of arbitrarily selected particles of the samples (A1–A4) are shown in Fig. 2. The SEM images of the samples show the formation of the regular spherical nanoparticle. The noticeable particle size by SEM differs from the calculated XRD due to the fact, the XRD crystallite sizes are the mean of the several crystallographic orientations whereas the particle size by SEM is maybe shaped by several crystallites. As well, the EDS patterns of randomly selected particle of the sample A1-A4 are presented in Fig. 2. The EDS patterns confirm the presence of Ag, In, Nb and O ions without any impurities. To ensure the homogeneity and dispersion of the elements, the element mapping was employed for the randomly selected areas of samples (A1–A4) along with point selection of A4. The elemental map shows the concentrations of Ag, In, Nb and O ions which suggest that integrated all the elements are present and they are distributed uniformly (Supplementary information) which further confirms the purity of the sample. EDS profile with elemental X-ray maps reveal that the sol-gel method is extremely effective to prepare the multifunctional nanostructures.

3.3. Thermal analysis

Thermal stability of the materials is one of the key parameters for determining their commercial applications. The DTA curves of the samples are shown in Fig. 3. In high temperature, only the sample A4 show a broad exothermic peak at 538 °C which implies that oxidation process may remove oxygen vacancy in the system. Better thermal stability was observed for the samples with a small endothermic peak at 966 °C.